Ultralow NEP in Hot-Electron Titanium Nanobolometers

Jian Wei[‡], David Olaya[‡], Sergei Pereverzev, Boris S. Karasik[§], Jonathan H. Kawamura, William R. McGrath, Andrei V. Sergeyev, and Michael E. Gershenson

***Abstract*—We have developed a hot-electron superconducting transition-edge sensor (TES) that is capable of counting THz photons and operates at $T = 0.3$K. We fabricated superconducting Ti nanosensors with Nb contacts with a volume of ~ 3×10^{-3} μm^3 on planar Si substrate and have measured the thermal conductance due to the weak electron-phonon coupling in the material $G = 4\times10^{-14}$ W/K at 0.3 K. The corresponding *NEP* = 3×10^{-19} W/Hz$^{1/2}$. This Hot-Electron Direct Detector (HEDD) is expected to have a sufficient energy resolution for detecting individual photons with $\nu > 1$ THz where NEP ~ 3×10^{-20} W/Hz$^{1/2}$ is needed for space spectroscopy.**

***Index Terms*—radiation detectors, submillimeter wave detectors, bolometers, superconducting devices**

I. Introduction

SEVERAL advanced space submillimeter astronomy missions (SAFIR [1,2], SPECS [3],SPICA [4]) have been recently proposed. These missions will make a dramatic impact on the achievable sensitivity in the spectrometer with moderate resolution ($R = \nu/\Delta\nu \sim 1000$) due to active cooling of telescope mirrors down to ~ 4 K. This deep cooling would significantly reduce the telescope emissivity and enable realization of the background-limited noise equivalent power (*NEP*) ~ 10^{-19}-10^{-20} W/Hz$^{1/2}$ at submillimeter wavelengths (see Fig. 1). However, the *NEP* of state-of-the-art direct detectors [2,5] needs to be lowered by almost two orders of magnitude to meet this goal. The membrane supported bolometers have come close to meeting the sensitivity goals [6]: a low phonon conductance has been achieved in long (~ 8 mm) Si_3N_4 beams suggesting an *NEP* ~ 10^{-19} W/Hz$^{1/2}$ in the 50-100 mK temperature range. The further decrease of the thermal conductance is hindered by the weakening of the temperature dependence of the thermal conductance due to transition to ballistic phonon transport.

Besides the more traditional photon-integrating mode of operation, a photon counting mode may be required to achieve the lowest *NEP*. Background-limited operation above 1 THz would correspond to a very low photon arrival rate [7]:

$$N_{ph} = \frac{1}{2}\left(\eta\frac{NEP}{h\nu}\right)^2 < 100\ \mathrm{s}^{-1}, \qquad (1)$$

(η is the optical coupling efficiency). A detector with a time constant τ will integrate a photon flux if $N_{ph}\tau >> 1$. Therefore, a background limited integrating detector must have a time constant of 0.1 s or greater. Such a long time constant is problematic for many detector concepts: typically, τ does not exceed a few milliseconds for hot-electron detectors and kinetic inductance detectors, so they both would have to operate in the photon counting mode for the detection of weak signals. Although the photon counting mode in the THz range has been considered in several papers (see, e.g., [7,8,9]), the detection of individual THz photons has been demonstrated only using the quantum-dot devices [10]. The latter approach has been recently advanced towards practical application in terahertz microscopy [11]. The drawback of the quantum-dot detector for space applications is a necessity to use strong magnetic field for the most sensitive operation and the lack, at present, of a multiplexed readout for a large array of such detectors.

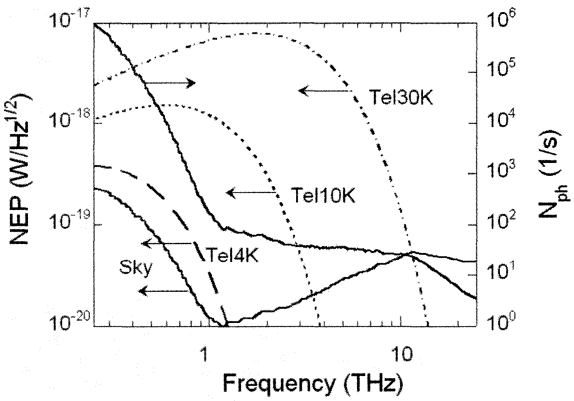

Fig. 1. The NEP limited by the background and by the telescope emission (5% emissivity, mirror temperature 4K, 10K, and 30K) for a moderate resolution spectrometer ($R = 1000$, single mode) and the arrival rate for background photons. The latter is less than 100 s^{-1} above 1 THz. Below 1 THz, the major contribution is due to the Cosmic Microwave Background radiation; at higher frequencies, radiation from the galactic core and dust clouds dominates.

II. Hot-Electron Direct Detector

We are pursuing a Hot-Electron Direct Detector (= hot-electron TES), which can operate in both photon-integrating

Manuscript received May 11, 2006. The work at Rutgers was supported in part by the NASA grant NNG04GD55G and the Rutgers Academic Excellence Fund. The research of BSK, JHK and WRM was carried out at the Jet Propulsion Laboratory, California Institute of Technology, under a contact with the National Aeronautics and Space Administration.

J. Wei, D. Olaya, S. Pereverzev and M. Gershenson are with Rutgers University, Piscataway, NJ 08854, USA.

B. Karasik, J. Kawamura, and W. McGrath are with the Jet Propulsion Laboratory, California Institute of Technology, Pasadena, CA 91109, USA.

A. Sergeyev is with SUNY ay Buffalo, Buffalo, NY 14260.

‡ These authors contributed equally to this work.

§ Corresponding author. Phone: 818-393-4438, email: boris.s.karasik@jpl.nasa.gov

and photon-counting modes at 0.3 K [12]. The idea of improving the sensitivity of bolometers by employing the hot-electron effects at ultra-low temperatures has been developed by several groups over a number of years [7,13,14,15,16]. The fundamental limit of the *NEP* is set in this case by the thermal energy fluctuations:

$$NEP = \sqrt{2k_B T_e^2 C_e(T_e,V)/\tau_{e-ph}(T_e)} \ . \qquad (2)$$

Here $C_e = \gamma V T_e$ is the electron heat capacity, V is the sensor volume, γ is the Sommerfeld constant, and $\tau_{e\text{-}ph}$ is the electron-phonon energy relaxation time. The sensitivity increases with decreasing the sensor volume and lowering the electron temperature T_e. Especially strong is the effect of lowering T_e: $NEP_{e\text{-}ph} \sim T_e^{7/2}$ because of a very rapid increase of the electron-phonon relaxation time $\tau_{e\text{-}ph} \propto T_e^{-4}$ in disordered conductors at ultra-low temperatures (see, e.g., [17,18]). Since the electron temperature is always ~ T_C in hot-electron TES, then lowering T_e requires reducing T_C to the desired level. This can be achieved by magnetic ion implantation, e.g. $^{+}Mn^{55}$ ions work well on Ti [19]. Using conventional nanolithographic methods, the volume of metallic nanostructures can be reduced down to ~10^{-21} m^3,

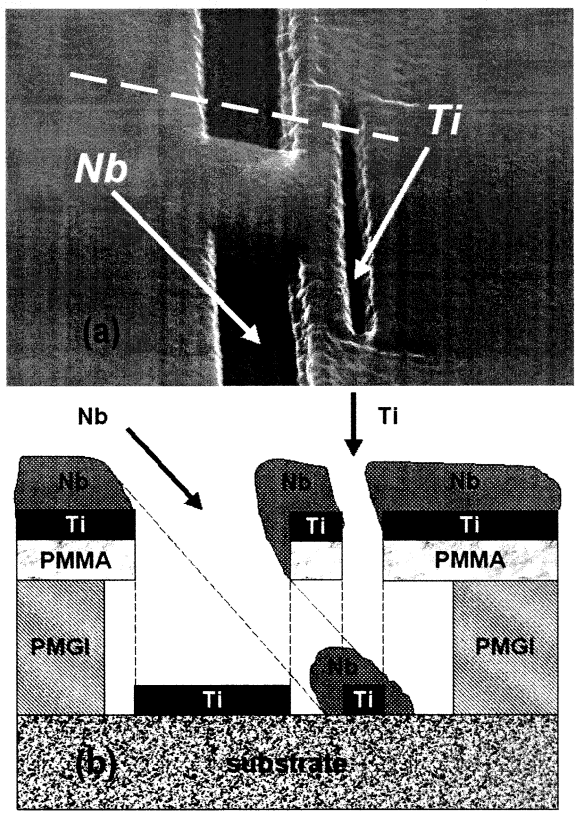

Fig. 2. (a) Shadow mask used for the fabrication of Ti HEDDs (the SEM picture has been taken after the deposition of Ti and Nb films). The arrows show the directions in which Nb and Ti were deposited. (b) Cross section along the dashed line on panel (a). A two-layer lift-off mask consists of the top 0.1-μm-thick PMMA layer, used as a high-resolution electron resist, and the bottom 0.3-μm-thick layer of polymer PMGI. A deep undercut in the bottom layer allows for the overlap of the films deposited at different incident angles: Ti is deposited along the direction normal to the plane of a substrate; Nb is deposited at 45° incidence angle and perpendicular to the long dimension of the 1-μm-long slit.

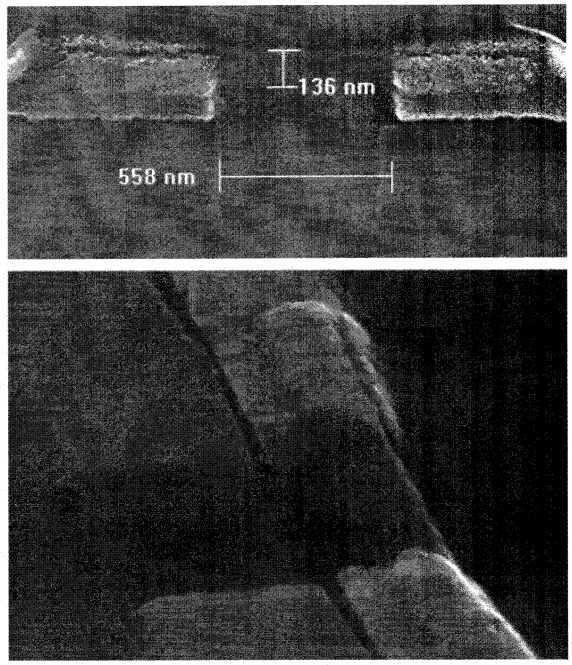

Fig. 3. SEM image of a Ti nanosensor. Top view: the Ti nanosensor with dimensions 0.04μm × 0.14μm × 0.56μm is flanked by Nb current leads (Ti is dark gray and Nb is light gray). The rest of Ti film is separated from the Ti nanosensor and Nb leads by trenches, which are clearly seen on the bottom microphotograph taken at an angle.

which translates into $C_e(0.3\,\mathrm{K}) \sim 10^{-19}$ J/K. For such a nanosensor, the predicted *NEP* can be 10^{-19} W/Hz$^{1/2}$ at $T \approx 0.3$ K and 10^{-20} W/Hz$^{1/2}$ at $T \approx 0.1$ K [12]. However, even a record long $\tau_{e\text{-}ph} \sim 20$ ms measured in thin Hf and Ti films at 40 mK [18] is insufficiently long for integrating photons with $N_{ph} \sim 100$ s^{-1}.

Equation (2) assumes that the electron-phonon relaxation is the only mechanism of energy dissipation. To prevent the energy flow from the antenna-coupled nanosensor, the electrical leads to the nanostructure should be made of a superconductor with a sufficiently large superconducting gap: in this case, while electrical current can freely flow across the normal metal-superconductor interface, the outdiffusion of "hot" electrons is blocked by Andreev reflection. The detector design should also ensure the suppression of photon emission by electrons in the frequency range corresponding to the operating temperature 0.3K (~ 10 GHz) [20]; this, however, can be achieved simultaneously with a good impedance match between the sensor and the embedded circuit.

We have been systematically working on the realization of ultra-sensitive HEDDs for a number of years [12,18,21,22] and recently achieved the expected thermal characteristics in nanoscale Ti HEDDs with Nb Andreev contacts.

A. Fabrication procedure

The HEDD element is a transition edge nanosensor made from thin Ti film with superconducting transition temperature T_C~0.2-0.4 K. The current leads to the nanosensor are fabricated from Nb films with $T_C \sim 8.5$ K; a large superconducting gap in Nb blocks outdiffusion of "hot" electrons to the current leads. The nanostructure is fabricated on a silicon substrate using electron-beam

lithography and e-gun deposition of Ti and Nb. For the fabrication of an oxide-free Ti/Nb interface, we have used the so-called "shadow mask" technique: Ti and Nb films were sequentially deposited at different angles through a "shadow" mask without breaking vacuum. An SEM image of a "shadow" mask is shown in Fig. 2. After developing the resist, the substrates were mounted in an oil-free deposition system with a base pressure ~1×10^{-9} mbar equipped with a cryo-pump and sorption pumps. To reduce substrate/resist heating in the process of deposition of Nb (melting $T = 2468$°C), the substrate holder was positioned at a large distance from the e-gun source (~ 40 cm). The substrate holder can tilt the substrate at an angle with respect to the direction to the e-gun source. Thin Ti film was deposited at a deposition rate ~1.5-3 nm/s along the direction normal to the plane of the substrate, Nb was deposited at a rate 0.5 nm/s along the direction which was at a 45° angle to the substrate and perpendicular to the long dimension of the nanosensor. Because the resist thickness exceeds the width of the narrow channel, Nb film covers only the ends of the Ti nanosensor.

A Ti device with typical dimensions is shown in Fig. 3. Among different tested devices the normal-state resistance ranges between 50-100 Ohm and the critical temperature is between 0.2-0.4 K. The minimum device width is set by the e-beam lithography. Further reduction of the device length is problematic: for nanosensors with length comparable to the thermal length $L_C = \sqrt{\hbar D / k_B T}$, where D is the diffusion constant, the superconducting transition temperature will be significantly increased due to the proximity effect between Ti nanosensor and Nb current leads. For the studied Ti films with diffusion constant $D \sim 4$ cm^2/s, L_C is of the order of 0.1 μm at $T = 0.3$K. Also, if the length of the Ti nanosensor is smaller than the electron thermalization length, the frequency-dependent response and drop in sensitivity might be expected at $h\nu > \Delta$Nb ($\nu > 0.3$ THz). For this reason we do not make HEDD devices shorter than ~ 0.5 μm.

B. Measurement of the thermal conductance

Measurements of the thermal conductance G have been performed in the dilution refrigerator equipped with several stages of low-pass electical filters thermally anchored to the 1K pot and mixing chamber; the filters were designed to suppress both the low-frequency interferences and rf noise over the frequency range from kHz to several GHz. Because of high sensitivity, the devices can be overheated above their superconducting transition temperature by electromagnetic noise with the power $\delta T_C C_e/\tau_{e\text{-}ph} \le 1$ fW.

Figure 4 illustrates the measurement of the thermal conductance $G = C_e/\tau_{e\text{-}ph}$ between the electrons in a nanosensor and the thermal bath. The resistance of devices was measured by an AC (13 Hz) resistance bridge using a small (typically, 0.1-1 nA) measuring current. The Ti nanosensor was slightly heated by a DC current, and the difference between the electron temperature T_e and the equilibrium bath temperature T_{ph} was determined by observing the temperature shift of the superconducting transition. This method assumes that the non-equilibrium electron distribution function can be characterized with an effective electron temperature. This assumption is valid at

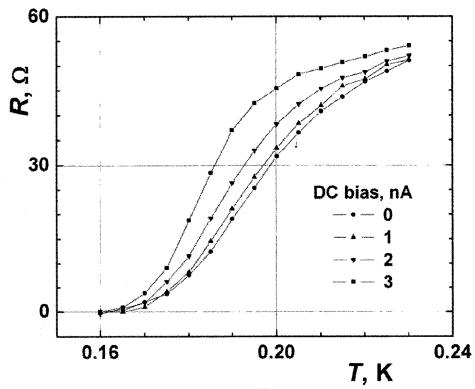

Fig. 4. Measurements of the thermal conductivity between the electrons in a Ti HEDD device with dimensions 0.04μm × 0.14μm × 0.56μm and the thermal bath. The shift of the superconducting transition is caused by the Joule heat generated in the sample by the DC bias current.

sub-Kelvin temperatures, where the electron-electron scattering rate in thin films exceeds by many orders of magnitude the electron-phonon scattering rate [13]. To measure G at $T < T_C$ the superconducting transition was suppressed to lower temperatures by applying a magnetic field perpendicular to the plane of the nanosensor. The thermal conductivity was found from the balance equation:

$$RI_{DC}^2 = G(T_e)(T_e - T_{ph}), \qquad (3)$$

which holds if $T_e - T_{ph} << T_{ph}$. For the device with dimensions 0.04μm × 0.14μm × 0.56μm (Fig. 3), we obtained $G(0.3\text{K}) = 4\times10^{-14}$ W/K. The value of G normalized to volume $G(0.3\text{K})/V = 1.2\times10^7$ W/(K·m^3) agrees very well with the corresponding value of G/V measured for much larger meander-patterned Ti films with dimensions 0.04μm × 5μm × 100,000μm (note that the length of 10 cm for the latter structures is much greater than the diffusion length over the electron-phonon relaxation time, $L_{e\text{-}ph} = (D\tau_{e\text{-}ph})^{1/2}$). The scaling of G with the sensor volume (over 6 orders of magnitude) provides an experimental proof that in both types of structures, the nanostructures with superconducting contacts and much larger Ti meanders, the dominant mechanism of energy dissipation at $T = 0.3$K is electron-phonon scattering, and that the energy relaxation due to outdiffusion of hot electrons can be neglected. The measured values of G are in good agreement with the estimate of G on the basis of the theory of electron-phonon energy relaxation in disordered conductors [17] and our previous measurements of the electron-phonon relaxation rate in disordered Ti films [18].

C. Modeling of the device performance

The Ti HEDD will operate in the voltage-biased TES mode; that is, its operating temperature will be somewhat lower than T_C, and the resistance at the operating point, R, will be much smaller than the normal resistance R_N. This biasing mode enables the device to simultaneously match to the antenna impedance and couple well to the SQUID. Indeed, if the DC resistance at the operating point is ~ 1 Ω, the device Johnson noise would exceed the noise of a typical DC SQUID; at the same time, a much higher impedance of

the device in the THz range (~ 50-100 Ω) facilitates coupling of the device to a planar antenna. The signal photon will be absorbed and increase the electron temperature in the nanosensor. The increase in electron temperature will cause the current to decrease, and will be registered by the SQUID-based readout. The response time of these devices is controlled by the electron-phonon energy relaxation time $\tau_{e\text{-}ph}$ (~5-20 μs at 0.3K, depending on disorder in Ti films and substrate material). If necessary, the response time can be further reduced by using the negative electrothermal feedback (ETF) [23]: $\tau = \tau_{e\text{-}ph}/(1+L)$, where L is the ETF loop gain.

In the photon integrating mode, the thermal-fluctuations-limited *NEP* for the developed HEDD with dimensions 0.04μm × 0.1μm × 0.5μm will be less than 3×10^{-19} W/Hz$^{1/2}$ at 0.3 K (see Eq. 2).

Since the time constant of the detector is not sufficiently long to integrate the background photons arriving at a rate < 100 s^{-1}, the photon-counting mode should be used to achieve the highest sensitivity at $\nu > 1$ THz. This case has been considered some of us earlier [7]. The analysis show that for the device with dimensions 0.04μm × 0.1μm × 0.5μm, the energy resolution at 0.3K, δE, corresponds to the "red boundary" $\nu_R = \delta E/h$ = 0.24 THz. The dynamic range $(\tau\ N_{ph}^{1/2})^{-1} \sim 50$ dB ($N_{ph}^{1/2}$ is the minimum signal which can be distinguished from the background) and the detector *NEP* at 1 THz is less than 10^{-20} W/Hz$^{1/2}$ if the discrimination threshold $E_T \approx 3.5\delta E$.

III. Conclusion

We have demonstrated a superconducting Hot-Electron Direct Detector with a record-low *NEP* = 3×10^{-19} W/Hz$^{1/2}$ at 0.3 K. This operating temperature can be achieved by He3 sorption cooling; for comparison, similar sensitivity in the conventional bolometers can be realized only at 0.1K or below, which requires dilution refrigeration or adiabatic demagnetization cooling techniques. In its most sensitive photon counting mode, this detector would be suitable for a background limited spectrometer with moderate resolution (R~1000) for SAFIR and other space-born far-IR telescopes with cryogenically cooled mirrors. For higher background applications (e.g., CMBPol), HEDD offers the background limited sensitivity at $T = 0.3$K. The hot-electron detectors have two other important advantages: (a) they are fabricated on bulk substrates, and (b) they have a very short time constant allowing for a high data rate. The HEDDs can be readily matched to a planar antenna since the device RF impedance is in the range 50-100 Ω and the device size is much smaller than the wavelength. As with other transition-edge sensors, the HEDD is compatible with SQUID-based multiplexing read-out circuits

References

[1] http://safir.jpl.nasa.gov/technologies.shtml.

[2]. D.J. Benford and S.H. Moseley, "Cryogenic detectors for infrared astronomy: the Single Aperture Far-InfraRed (SAFIR) Observatory," *Nucl. Instr. Meth. Phys. Res. A* 520(1-3), 379-383 (2004).

[3]. D. Leisawitz, "NASA's far-IR/submillimeter roadmap missions: SAFIR and SPECS," *Adv. Space Res.* 34(3), 631-636 (2004).

[4]. T. Nakagawa, "SPICA: space infrared telescope for cosmology and astrophysics," *Adv. Space Res.* 34(3), 645-650 (2004).

[5] J.J. Bock, P. Day, A. Goldin, H.G. LeDuc, C. Hunt, A. Lange et al., "Antenna-coupled bolometer array for astrophysics," *Proc. Far-IR, SubMM & MM Detector Technology Workshop, April 1-3, 2002, Monterey, CA*, 224-229.

[6] M. Kenyon, P.K. Day, C.M. Bradford, J.J.Bock, and H.G. Leduc, "Background-imited membrane-isolated TES bolometers for far-IR/submillimeter direct-detection spectroscopy," *Nucl. Instr. & Meth. Phys. Res. A* 559, 456-458 (2006).

[7] B.S. Karasik and A.V. Sergeev, "THz Hot-Electron Photon Counter," *IEEE Trans. Appl. Supercond.* 15(2), 618-621 (2005).

[8] R.J. Schoelkopf S.H. Moseley, C.M. Stahle, P. Wahlgren, and P. Delsing, "A concept for a submillimeter-wave single-photon counter," *IEEE Trans. Appl. Supercond.* 9(2), Pt.3, 2935-2939 (1999).

[9] A. Semenov, A. Engel, K. Il'in, G. Gol'tsman, M. Siegel and H.W. Hubers, "Ultimate performance of a superconducting quantum detector," *Eur. Phys. J. Appl. Phys.* 21(3), 171-178 (2003).

[10] S. Komiyama, O. Astafiev, V. Antonov, T. Kutsuwa, and H. Hirai, "A single-photon detector in the far-infrared range," *Nature* 403, 405-407 (2000); O. Astafiev, S. Komiyama, T. Kutsuwa, V. Antonov, Y. Kawaguchi, and K. Hirakawa, "Single-photon detector in the microwave range," *Appl. Phys. Lett.* 80(22), 4250-4252 (2002); H. Hashiba, V. Antonov, L. Kulik, S. Komiyama, and C. Stanley, "Highly sensitive detector for submillimeter wavelength range," *Appl. Phys. Lett.* 85(24), 6036-6038 (2004).

[11] K. Ikushima, Y. Yoshimura, T. Hasegawa, S. Komiyama, T. Ueda, and K. Hirakawa, "Photon-counting microscopy of terahertz radiation," *App. Phys. Lett.* 88, 152110 (2006).

[12] B.S. Karasik, W.R. McGrath, M.E. Gershenson, and A.V. Sergeev, "Photon-noise-limited direct detector based on disorder-controlled electron heating," *J. Appl. Phys.* 87(10), 7586-7588 (2000).

[13] E. M. Gershenson, M. E. Gershenson, G. N. Goltsman, A. D. Semenov, and A. V. Sergeev, "Heating of electrons in a superconductor in the resistive state by electromagnetic radiation," *Sov.Phys.-JETP* 59, 442-450 (1984).

[14] M.Nahum and J.M. Martinis, "Ultrasensitive hot-electron microbolometer," *Appl. Phys. Lett.* 63, 3075-3077 (1993).

[15] B. Cabrera, R.M. Clarke, P. Colling, A.J. Miller. S. Nam, R.W. Romani, "Detection of single infrared, optical, and ultraviolet photons using superconducting transition edge sensors," *Appl. Phys. Lett.* 73(6), 735-737 (1998).

[16] T.A Lee, P.L. Richards, S.W. Nam, B. Cabrera, and K.D. Irwin, "A superconducting bolometer with strong electrothermal feedback," *Appl. Phys. Lett.* 69, 1801-1803 (1996).

[17] A. Sergeev and V. Mitin, "Electron-phonon interaction in disordered conductors: Static and vibrating scattering potentials," *Phys. Rev. B.* 61(9), 6041-6047 (2000).

[18] M.E. Gershenson, D. Gong, T. Sato, B.S. Karasik, A.V. Sergeev, "Millisecond electron-phonon relaxation in ultrathin disordered metal films at millikelvin temperatures," *Appl. Phys. Lett.* 79, 2049-2051 (2001).

[19] B.A. Young, J.R. Williams, S.W. Deiker, S.T. Ruggiero, and B. Cabrera, "Using ion implantation to adjust the transition temperature of superconducting films," *Nucl. Inst. Meth. Phys. Res. A* 520, 307-310 (2004).

[20] D.R. Schmidt, R.J. Schoelkopf, and A.N. Cleland, "Photon-Mediated Thermal Relaxation of Electrons in Nanostructures," *Phys. Rev. Lett.* 93, 045901 (2004).

[21] B.S. Karasik, B. Delaet, W.R. McGrath, J. Wei, M.E. Gershenson, and A.V. Sergeev, "Experimental Study of Superconducting Hot-Electron Sensors for Submm Astronomy," *IEEE Trans. Appl. Supercond.* 13(2), 188-191 (2003).

[22] B.S. Karasik, A.V. Sergeyev, D. Olaya, J. Wei, M.E. Gershenson, J.H. Kawamura, and W.R. McGrath, "A Photon Counting Hot-Electron Bolometer for Space THz Spectroscopy," *Proc. 16th Int. Symp. Space Terahertz Technol., May 2-4, 2005, Gothenburg, Sweden*, 543-548.

[23] K.D. Irwin, "An application of electrothermal feedback for high resolution cryogenic particle detection," *Appl. Phys. Lett.* 66, 1998-2000 (1995).